

Shape and Core-Excited Resonances in Thiophene

Alexandra Loupas, Khrystyna Regeta, Michael Allan, and Jimena D. Gorfinkiel

J. Phys. Chem. A, **Just Accepted Manuscript** • DOI: 10.1021/acs.jpca.7b11865 • Publication Date (Web): 27 Dec 2017

Downloaded from <http://pubs.acs.org> on January 9, 2018

Just Accepted

“Just Accepted” manuscripts have been peer-reviewed and accepted for publication. They are posted online prior to technical editing, formatting for publication and author proofing. The American Chemical Society provides “Just Accepted” as a free service to the research community to expedite the dissemination of scientific material as soon as possible after acceptance. “Just Accepted” manuscripts appear in full in PDF format accompanied by an HTML abstract. “Just Accepted” manuscripts have been fully peer reviewed, but should not be considered the official version of record. They are accessible to all readers and citable by the Digital Object Identifier (DOI®). “Just Accepted” is an optional service offered to authors. Therefore, the “Just Accepted” Web site may not include all articles that will be published in the journal. After a manuscript is technically edited and formatted, it will be removed from the “Just Accepted” Web site and published as an ASAP article. Note that technical editing may introduce minor changes to the manuscript text and/or graphics which could affect content, and all legal disclaimers and ethical guidelines that apply to the journal pertain. ACS cannot be held responsible for errors or consequences arising from the use of information contained in these “Just Accepted” manuscripts.



Shape and Core-excited Resonances in Thiophene

Alexandra Loupas,^{†,‡} Khrystyna Regeta,^{¶,§} Michael Allan,[¶] and Jimena D.

Gorfinkiel^{*,‡}

[†]*Departamento de Física, Faculdade de Ciências e Tecnologia, Universidade Nova de Lisboa, Campus de Caparica, 2829-516, Portugal*

[‡]*School of Physical Sciences, The Open University, Walton Hall, Milton Keynes, MK7 6AA, United Kingdom.*

[¶]*Department of Chemistry, University of Fribourg, Fribourg, 1700, Switzerland*

[§]*Current address: Departamento de Física, Faculdade de Ciências e Tecnologia, Universidade Nova de Lisboa, Campus de Caparica, 2829-516, Portugal*

E-mail: jimena.gorfinkiel@open.ac.uk

Abstract

We present a comprehensive study of resonance formation in electron collisions with thiophene. Detailed calculations have been performed using the *ab initio* R-matrix method. Absolute differential cross sections for electron impact excitation up to 18 eV and for two scattering angles, 90° and 135°, have been measured. Agreement between the calculated and measured experimental cross sections is very good. Three shape resonances previously described, two of π^* character and one σ^* , as well as a number of resonances of core-excited or mixed character are identified and characterized in the calculations. The measured cross sections provide experimental confirmation for a number of the core-excited resonances. The link between these resonances and prior DEA experiments is discussed.

Introduction

The impact of low energy electrons is well known to cause bond cleavages in DNA.¹ This break-up is initiated through the formation of a negative ion transient state, commonly known as a resonance. Depending on its characteristics, this anionic state will decay either via autodetachment or lead to dissociation and the formation of two or more fragments, one of them negatively charged, during a process known as dissociative electron attachment (DEA).² Free and pre-solvated electrons are formed in large quantities when radiation interacts with biological matter.³ Therefore, understanding DEA and resonance formation is crucial to the interpretation of how low-energy electrons induce DNA damage: a lot of work has been performed, both theoretical and experimental, specially on DNA constituents (in particular nucleobases), some aminoacids, radiosensitizers and model molecules.^{4,5}

This work presents the study of low energy electron collisions with thiophene (C₄H₄S), one of the most used building blocks in anti-inflammatory drugs.⁶ Thiophene is a prototypical, fully conjugated, heterocyclic molecule which contains one heavy and highly polarizable sulfur atom. Thiophene is also the main unit of several types of materials, as polythio-

1
2
3 phene. When properly doped, polythiophene is conductive and has found application in
4 electrochromic displays, electro-optic devices, protection against photocorrosion and energy
5 storage.⁷ In other materials, thiophene's presence confers various important properties, mak-
6 ing them promising as photochromatic molecular switches,⁸ organic semiconductors,⁹ solar
7 cells,¹⁰ light-emitting diodes and field-effect transistors.¹¹ As all of these applications in-
8 volve electron transfer, understanding thiophene's electronic structure and electron induced
9 processes is of great relevance.

10
11
12
13
14
15
16
17
18
19
20
21
22
23
24
25
26
27
28
29
30
31
32
33
34
35
36
37
38
39
40
41
42
43
44
45
46
47
48
49
50
51
52
53
54
55
56
57
58
59
60

Electron collisions with thiophene have been previously studied both at theoretical and experimental levels. The only DEA study was performed by Muftakhov *et al.*¹² who recorded mass spectra in the gas phase in the energy range 0-12 eV. They interpreted the peaks in these spectra as corresponding to 7 resonant states mainly of Feshbach character, a couple of which lie above the ionization threshold and therefore are expected to correspond to core-excited resonances in which the electron is excited from a deeply bound orbital.

Asmis¹³ measured electron energy loss spectra (EELS) for vibrational excitation and found three resonances at 1.27, 2.83 and 5.5 eV. He assigned the first two resonances as 1 particle (i.e. shape) π^* resonances and the last one as a σ^* resonance.¹

Modelli and Burrow¹⁴ obtained electron transmission spectra (ETS) for thiophene below $\simeq 4.5$ eV. They found two intense resonances at 1.15 and 2.63 eV, associated with electron capture into the two lowest empty π^* molecular orbitals, of b_1 and a_2 symmetry. They stated the signal corresponding to an expected σ^* resonance (scaled virtual orbital energies in their work put the σ^* resonance around 2-2.1 eV) is probably masked by overlap with the high-energy tail of the lower, more intense π^* resonance.

Hedhili *et al.*⁷ investigated electron stimulated desorption (ESD) of anions from multi-layer thiophene condensed on a polycrystalline platinum substrate. The yield functions they obtained show that anions are desorbed both by dissociative electron attachment, with peaks observed at 9.5, 11 and 16 eV, and for higher energies, via dipolar dissociation.

¹A summary of the EELS can be found here: http://homeweb.unifr.ch/allanm/pub/ma/dir_allan/thiophene_EELS.PDF

1
2
3 From the theoretical point of view, two methods have been applied to the study of
4 electron scattering from thiophene at low energies. Firstly, da Costa *et al.*¹⁵ reported electron
5 impact integral elastic, momentum transfer and differential cross sections calculated with the
6 Schwinger multichannel method with pseudopotentials (SMCPP) for energies ranging from
7 0.5 to 6 eV. They identified two π^* and a σ^* shape-resonances, the latter with a strong *d*-wave
8 character. Vinodkumar *et al.*¹⁶ used the R-matrix method (through the QUANTEMOL-N
9 interface) for low energy calculations and the Spherical Complex Optical Potential formalism
10 for intermediate to high energy. Their R-matrix calculations are similar to those presented
11 in this paper, however, their results (see later) are very different and show a number of
12 inconsistencies. No work has focused on core-excited resonances. Finally, we note that
13 Mozejko *et al.*¹⁷ calculated integral elastic and ionization cross sections at intermediate
14 and high electron-impact energies using the additivity rule approximation and the binary-
15 encounter-Bethe approach.
16
17
18

19 In this work, we have investigated resonance formation in thiophene both experimentally
20 and computationally. We have used the R-matrix method,¹⁸ as implemented in the UKRmol
21 suite¹⁹ to investigate electron collisions with thiophene in its equilibrium geometry. We have
22 performed the calculations at different levels of complexity to identify and characterized both
23 shape and core-excited resonances. We have also determined excitation function (i.e. angular
24 differential cross sections as a function of incident electron energy for a specific energy loss)
25 by means of EELS. Both the calculated data and the detailed excitation functions show the
26 presence of a number of mixed and core-excited resonances, some of which can be correlated
27 with peaks in DEA anion yields.¹²
28
29
30
31
32
33
34
35
36
37
38
39
40
41
42
43
44
45
46
47
48
49
50
51
52
53
54
55
56
57
58
59
60

Theory

The R-matrix method

We performed our scattering calculations within the fixed-nuclei approximation, that is, keeping the nuclei fixed at the ground state equilibrium geometry of the molecule. The R-matrix method has been described in detail elsewhere,^{18,20} so we present only a brief description here.

The basic idea of this method is the division of the configuration space into two regions, separated by a sphere of radius a , the R-matrix sphere. In the inner region, correlation and exchange effects between all electrons play a crucial role and have to be considered. In the outer region, exchange between the scattering electron and the electrons of the target system can be neglected. It is crucial for the applicability of the method that the radius of the R-matrix sphere is chosen in a way that contains the charge densities of the relevant target electronic states and the $N + 1$ electron functions χ_i defined below.

In the inner region, we describe the system using a set of basis functions Ψ_k of the form:

$$\Psi_k = \mathcal{A} \sum_{i=1}^n \sum_{j=1}^{n_c} \Phi_i(\mathbf{x}_N; \hat{r}_{N+1}; \sigma_{N+1}) \frac{u_{ij}(r_{N+1})}{r_{N+1}} a_{ijk} + \sum_{i=1}^m \chi_i(\mathbf{x}_{N+1}) b_{ik} \quad (1)$$

where \mathcal{A} is the antisymmetrization operator; Φ_i are the wavefunctions describing the target electronic states and \mathbf{x}_N and \mathbf{x}_{N+1} represent spin and space coordinates of all N and $N + 1$ electrons, respectively. σ_{N+1} stands for the spin of the $(N + 1)$ th scattering electron and r_{N+1} and \hat{r}_{N+1} for its radial and angular coordinates, respectively. The functions $\frac{u_{ij}(r_{N+1})}{r_{N+1}}$ describe the radial part of the wavefunction of the scattering electron while the L^2 integrable functions χ_i are necessary for a good description of the short-range polarization-correlation effects. Finally, the coefficients a_{ijk} and b_{ik} are determined by the requirement that the functions Ψ_k diagonalise, in the inner region, the electronic non-relativistic Hermitian Hamiltonian of the $(N + 1)$ -electron system.²⁰

In the outer region, the wavefunction describing the scattering electron is approximated

1
2
3 by a single-centre, partial wave expansion, reducing drastically the computational cost. Hav-
4 ing obtained the basis functions Ψ_k , the R-matrix is built and propagated to the asymptotic
5 region, where the K-matrix is obtained. From the K-matrix, one can determine the S-matrix
6 and, from it, the cross sections. Both K- and S-matrices can be used to identify and charac-
7 terize resonances.
8
9

10
11
12
13 In our study we included partial waves up to $l = 4$ (and tested, for the smaller cal-
14 culations, $l = 5$). Inclusion of higher partial waves increases the computation cost of the
15 calculations significantly. Additionally, this partial wave expansion does not converge in the
16 fixed-nuclei approximation for polar molecules. This lack of convergence is usually circum-
17 vented by means of a Born correction.²¹ However, given the relatively small dipole moment
18 of thiophene (see below), we have not included this correction: it only affects dipole allowed
19 transitions and the effect for electronic excitation in the energy range of interest has been
20 shown to be small (around 5%) even for molecules with a much larger dipole moment (for
21 example, pyridine²² with $\mu=2.33$ Debye). The effect of not including the correction will be
22 to underestimate the elastic and total cross sections, most visibly at low energies and the
23 cross sections for excitation into singlet states at higher energies.
24
25
26
27
28
29
30
31
32
33
34

35 Angular differential cross sections for electronic excitation are calculated following a well
36 established methodology based on the adiabatic nuclei approximation^{23,24} using a program
37 developed by Z. Mašín. The approach uses the T-matrix (trivially obtained from the S-
38 matrix) calculated with the R-matrix method.
39
40
41
42

43 Different levels of approximation can be employed in scattering calculations and these
44 are determined by the choice of of target electronic states (how many) and the type of the
45 L^2 functions included in the expansion (1). The Static-Exchange (SE) and Static-Exchange
46 plus Polarization (SEP) approximations use a Hartree-Fock description of the ground elec-
47 tronic state of the target, the only state included in the calculation. These approximations
48 are capable of describing resonances in which the target molecule remains in the ground
49 state, known as shape resonances. In the SEP approximation, the molecule is allowed to be
50
51
52
53
54
55
56
57
58
59
60

polarized by the incoming electron. This effect is modelled by including the appropriate L^2 configurations:

$$\chi_i : (\textit{core})^{N_c}(\textit{valence})^{N-N_c}(\textit{virtual})^1 \quad (2)$$

$$\chi_i : (\textit{core})^{N_c}(\textit{valence})^{N-N_c-1}(\textit{virtual})^2 \quad (3)$$

where the core orbitals are always doubly occupied by N_c electrons. The valence space is defined here as those orbitals occupied in the ground state configuration that are not core orbitals. Single excitations from the valence to a selected number of virtual orbitals (VO), which are also available for the incoming electron, are allowed. Due to the presence of these single excitations from the valence space to a VO, the SEP model can sometimes describe (poorly) core-excited resonances.

The Close-Coupling (CC) method is necessary for the accurate description of core-excited resonances, i.e. resonances in which the electron excites the molecule as it attaches itself to it. In this case, wavefunctions corresponding to a number of excited states of the target are included in expansion (1). These are usually described at the Complete Active Space (CAS) level. Here, the L^2 configurations take the following form:

$$\chi_i : (\textit{core})^{N_d}(\textit{CAS})^{N-N_d+1}, \quad (4)$$

$$\chi_i : (\textit{core})^{N_d}(\textit{CAS})^{N-N_d}(\textit{virtual})^1. \quad (5)$$

where the active space (*CAS*) includes both occupied and unoccupied orbitals of the ground state configuration. Therefore, the virtual space is different to that of the SEP L^2 configurations; similarly, more orbitals are normally treated as core orbitals here to keep the size of the calculation feasible.

Whereas the choice of active space is guided by conventional computational chemistry considerations and the number of excited states to be included at CC level is determined by the range of scattering energies to be studied, choosing how many VO to include in the

1
2
3 above configurations is not straightforward: not enough VO will lead to a poor description
4 of polarization effects. Too many VO can lead to overcorrelation of the $N + 1$ wavefunctions:
5 in this case, resonances will appear lower in energy than they physically are. As we will see
6 later, the choice of VO has not been straightforward in this work.
7
8
9
10

11 **The time-delay analysis**

12
13 The main focus of this work is resonance identification and characterization. One common
14 way to find resonances is to look at the cross sections, although this approach is not always
15 reliable: peaks corresponding to physical resonances may be masked by other resonances
16 or the non-resonant contribution to the scattering processes and features that look like
17 peaks may not actually correspond to resonances. Another quantity that allows resonance
18 identification is the eigenphase sum, obtained from diagonalizing the K-matrix. It was shown
19 by Hazi²⁵ that an isolated resonance manifests itself as a characteristic jump of approximately
20 π in the eigenphase sum in the energy region centered around the position of the resonance.
21 However, resonances may also be difficult to identify in the eigenphase sum when they overlap
22 or the non-resonant contribution is significant.²⁶
23
24
25
26
27
28
29
30
31
32
33
34

35 Analysis of the time-delay enables the unambiguous identification of resonances even
36 in cases in which the eigenphase sum does not show the typical resonant behaviour. A
37 description of the method and its applications, as well as its advantages over the conventional
38 eigenphase sum analysis have been reviewed in detail before.²⁷
39
40
41
42

43 We use the definition of the time-delay as formulated by Smith:²⁸ the **Q**-matrix - the
44 time-delay matrix - at a given energy is calculated directly from the S-matrix:
45
46
47
48

$$49 \mathbf{Q}(E) = i\hbar\mathbf{S}\frac{d\mathbf{S}}{dE} \quad (6)$$

50
51
52 The process of searching for resonances involves the analysis of the positive eigenvalues
53 (time-delays) and associated eigenvectors of the **Q**-matrix for each energy. Resonances ap-
54
55
56
57
58
59
60

1
2
3
4
5
6
7
8
9
10
11
12
13
14
15
16
17
18
19
20
21
22
23
24
25
26
27
28
29
30
31
32
33
34
35
36
37
38
39
40
41
42
43
44
45
46
47
48
49
50
51
52
53
54
55
56
57
58
59
60

appear as a Lorentzian peak in these eigenvalues. Those time-delays much larger than \hbar/E can be interpreted as arising from resonant processes and can be fitted using:

$$\frac{\hbar\Gamma_\alpha}{(E - E_\alpha)^2 + (\Gamma_\alpha/2)^2} + 2\hbar\frac{d\delta_{bg}}{dE} \quad (7)$$

where E_α and Γ_α are, respectively, the position and width of resonance α and δ_{bg} is the background contribution to the eigenphase sum, weakly dependent on energy.

The analysis of the time-delay also allows us to characterize the resonances in terms of their parent state(s). The square of the j -th coefficient of the eigenvectors of $\mathbf{Q}(E)$ corresponding to a resonance ($|c_j|^2$) is equal to the branching ratio, which gives the probability of decay of a metastable state into the j -th channel, and consequently, can be used to determine the parent states of shape and core-excited shape resonances.

In this work, we used the inspection of the time-delay to identify and characterize all resonances.

Experimental approach

EELS and measurements of energy dependence spectra (also called excitation functions) were performed using a well tested spectrometer with hemispherical analyzers^{29,30} and employing procedures used previously to study electron scattering from targets like furan³¹ and pyrimidine.^{32,33} The spectrometer uses hemispherical analyzers to improve resolution. The electron beam current was 300-700 pA. The energy of the incident electrons was calibrated on the 19.365 eV ²S resonance in helium³⁴ and is accurate to within ± 10 meV. The sensitivity of the instrument depends on the electron energies. This effect, expressed as the instrumental response function, was quantified on elastic scattering in He; all our spectra were corrected as previously described.^{29,30} The technicalities of ‘tuning’ the instrument and of determining the response functions have been described in previous work^{29,30} particularly on N₂.³⁵

The absolute values of the excitation functions were determined by comparing the areas

1
2
3 under the elastic peak and under the electronic excitation bands of interest as previously
4 described.³¹ The required absolute values of the elastic cross sections (presented in the
5 supporting information) were determined by the relative flow technique as described by
6 Nickel *et al.*³⁶ using, as a reference, the theoretical helium elastic cross sections of Nesbet.³⁷
7
8 The confidence limit is $\pm 15\%$ for the elastic cross sections and $\pm 25\%$ for the inelastic cross
9 sections and excitation functions.
10
11
12
13
14
15
16

17 Computational details

18
19
20 Thiophene, C_4H_4S , is a planar molecule that belongs to the C_{2v} point group. It contains 44
21 electrons and has a dipole moment of 0.52 Debye.³⁸ Its experimentally determined polariz-
22 ability³⁹ is $60.8 a_0^3$ and its ionization energy is 8.86 eV.⁴⁰ Thiophene is an asymmetric top
23 and its first electronic excitation threshold is around 3.7 eV.^{13,41-43}
24
25
26
27

28 In our calculations, we have used the molecular geometry listed on the NIST website,
29 calculated at MP2 level using the cc-pVDZ basis set.⁴⁰
30
31
32
33

34 Target model

35
36
37 The electronic excited states of thiophene have been studied by a number of experimental
38 and theoretical groups. Flicker *et al.*⁴³ performed electron impact experiments at scattering
39 angles from 0° to 80° and impact energies of 30 and 50 eV, to study the lowest singlet-triplet
40 transitions of thiophene. Palmer *et al.*⁴¹ investigated the VUV and EELS spectra of thio-
41 phene, and assigned the bands by means of high level multi-reference multi-root CI studies,
42 with several basis sets. Haberkern *et al.*⁴² measured high-resolution EELS spectra in the
43 range of the low-lying singlet-triplet excitations. In combination with *ab initio* calculations,
44 the spectral structures were assigned and adiabatic transition energies were determined.
45
46 Salzmann *et al.*⁴⁴ used the time-dependent Kohn-Sham density functional theory combined
47 with a density functional/multi-reference configuration interaction method (DFT/MRCI) to
48
49
50
51
52
53
54
55
56
57
58
59
60

1
2
3 explore the ground and low-lying electronically excited states of thiophene, in order to ex-
4 plain the ultrafast decay of low-lying vibrational levels of the lowest singlet state, observed
5 by time-resolved pump-probe femtosecond multiphoton ionization spectroscopy.⁴⁵ Holland *et*
6 *al.*⁴⁶ used synchrotron radiation-based Fourier transform spectroscopy to study the excited
7 states of thiophene. A highly resolved photoabsorption spectrum was measured between
8 5 and 12.5 eV, combined with high-level *ab initio* calculations that used the second-order
9 algebraic-diagrammatic construction polarization propagation approach, and the equation-
10 of-motion coupled-cluster (EOM-CC) method at the CCSD and CC3 levels, to assign the
11 spectrum. Nakatsuji *et al.*⁴⁷ used the symmetry-adapted cluster configuration interaction
12 (SAC-CI) method and a basis set augmented with diffuse Rydberg functions to describe a
13 large number of Rydberg states. Merchán *et al.*⁴⁸ studied the electronic spectrum of thio-
14 phene using multiconfiguration second-order perturbation theory and extended ANO basis
15 set. Their results were used to assign the experimental spectrum below 8 eV. Kleinschmidt *et*
16 *al.*⁴⁹ used SPOCK (a code that calculates spin-orbit matrix elements in the one-center mean-
17 field approximation for multireference CI wave functions) and the DFT/MRCI approach to
18 provided excitation energies in good agreement with the experiments.

19
20 For our calculations, we tested two different basis sets: cc-pVDZ and 6-311G**. Since, as
21 prior work identified, thiophene possesses a significant number of low-lying Rydberg states,
22 the 6-311G** basis set produced results closer to experiments. Therefore, throughout this
23 work we present results obtained with this basis set. We note, however, that our calculations
24 do not describe the Rydberg states well.

25
26 Hartree-Fock SCF (HF) and state-averaged CASSCF orbitals were generated using MOL-
27 PRO⁵⁰ and used in the scattering calculations. In the state-averaged CASSCF calculations,
28 we used the active space of (10,9) (10 electrons distributed among 9 orbitals) and included
29 in our state-averaging 7 states: $1-2^1A_1$ $1-3^1B_1$ 1^1B_2 1^1A_2 . The ground state configuration of
30 thiophene is $1a_1^2 2a_1^2 1b_2^2 3a_1^2 2b_2^2 4a_1^2 3b_2^2 5a_1^2 1b_1^2 6a_1^2 7a_1^2 4b_2^2 8a_1^2 5b_2^2 9a_1^2 6b_2^2 10a_1^2 7b_2^2 2b_1^2 11a_1^2 3b_1^2 1a_2^2$. The
31 active space comprised the orbitals $11-12a_1$, $7-8b_1$, $2-4b_2$ and $1-2a_2$. The ground state ener-

gies and dipole moments obtained are, for the HF and CASSCF calculations, -551.343 and -551.428 Hartree, and 0.722 and 0.549 Debye.

Table 1 lists the vertical excitation energies of the 25 states (ground state + 24 excited states) included in the CC calculation together with the most relevant prior theoretical and experimental results. We observe that the agreement between our results and both theory and experiment gets worse as the energy increases. This agreement is reasonably good for the first few states, but differences of several eV occur for the higher states. We note that the calculations of Nakatsuji *et al.*⁴⁷ produce a large number of Rydberg states not described by ours: the more diffuse basis sets that would be needed to describe these states (and improve the description of other Rydberg states) would entail the use of much bigger radii. Unfortunately, with the UKRmol suite, this would lead to either serious linear dependence problems or a significant decrease in the quality of the continuum description.¹⁸ This poor and incomplete description of the Rydberg states in our calculations means that any resonances associated to them will either not be described or described poorly.

Scattering model

A radius of $15a_0$ was required for the R-matrix sphere for the calculation as the 6-311G** basis set was used. We included partial waves up to $l = 4$; the effect of adding $l = 5$ was tested at the SEP level and no significant changes were observed in the resonance positions. In the UKRmol suite, the continuum orbitals are Schmidt orthogonalised to the orbitals of the target: the resulting continuum orbitals face a symmetric orthogonalisation, where the deletion threshold was set to 1×10^{-7} .

We performed the calculations at SE, SEP and CC level freezing 9 and 17 core orbitals (i.e. $N_c=18$ and $N_d=34$ in expressions (3) and (4)), in the latter calculations respectively. For molecules with significant polarizability, a good description of the resonances (their position and width) depends strongly on the quality of the description of the polarization effects. As explained above, this depends on the number of VO included in the calculation, but,

Table 1: Calculated vertical excitation thresholds (in eV) of the electronic states included in the CC calculation. The energies of the states identified in our EELS spectra are indicated with *a*. Previous results are from: calculations, Salzmann *et al.*,⁴⁴ Kleinschmidt *et al.*,⁴⁹ Holland *et al.*,⁴⁶ Nakatsuji *et al.*⁴⁷ and Merchán *et al.*⁴⁸ (both CASSCF and PT2 results are presented); experiments, Moodie *et al.*,⁵¹ Zauli *et al.*,⁵² Flicker *et al.*,⁴³ van Veen *et al.*,⁵³ Asmis,¹³ Haberkern *et al.*⁴² and Veszpremi *et al.*⁵⁴ The energies labelled with a *R* correspond to Rydberg states. The vertical dots (:) indicate that several other states are present in that calculation in this energy range.

	Ours	44	49	46	47	CASSCF	PT2F	Exp.
1 ³ B ₂	3.722	3.53	3.39	-	3.94	3.83	3.75	3.7, ⁵³ 3.72 ^{13a} 3.75, ⁴³ 3.74 ^{41,42}
1 ³ A ₁	4.943	4.35	4.33	-	4.86	4.90	4.50	4.6, ⁵³ 4.61 ^a 4.62 ^{13,41-43}
1 ¹ A ₁	5.916	5.39	5.24	5.64	5.41	6.41	5.33	5.41 ^a ,5.43 ^{13,41,42} 5.45, ¹³ 5.48 ⁴³
1 ³ B ₁	6.371	5.65 _R	5.69	-	5.94 _R	5.93	5.90	5.9 ^a
1 ³ A ₂	6.457	5.77 _R	5.64	-	5.75 _R	5.57	5.88	5.9 ^a
1 ¹ B ₁	6.660	5.86 _R	5.88	6.17	5.87 _R	6.72	6.23	-
					⋮			
2 ³ A ₁	6.816	-	5.63	-	-	-	-	-
1 ¹ A ₂	6.877	5.88	5.72	6.23	6.41 _R	6.43	5.93	5.9, ⁴³ 6.0 ^{52,54}
2 ³ B ₂	6.906	-	5.99	-	-	-	-	-
1 ¹ B ₂	6.952	5.54	5.42	5.97	5.72	8.10	5.72	5.52, ⁴¹ 5.61 ^{13,42} 5.65, ⁵⁵ 5.77 ⁵¹
					⋮			
2 ¹ A ₁	8.060	-	7.03	7.38	6.73	8.85	6.69	6.6, ⁵³ 6.7 ⁵²
					⋮			
2 ¹ B ₂	9.411	-	-	6.97	6.41 _R	6.79	6.56	7.1 ⁴³
3 ³ A ₁	9.563	-	-	-	-	-	-	-
2 ³ A ₂	9.731	5.80 _R	-	-	-	-	-	-
2 ¹ A ₂	10.055	6.10 _R	6.33	-	6.73 _R	7.50	6.97	-
3 ³ B ₂	10.116	-	-	-	-	-	-	-
4 ³ B ₂	10.139	-	-	-	-	-	-	-
5 ³ B ₂	10.368	-	-	-	-	-	-	-
3 ¹ B ₂	10.630	-	-	7.69	7.12 _R	7.44	7.28	-
3 ¹ A ₁	10.749	-	-	7.65	7.32	7.46	7.23	-
2 ³ B ₁	10.827	-	6.18	-	-	-	-	-
3 ³ A ₂	11.046	-	6.11	-	-	-	-	-
6 ³ B ₂	11.247	-	-	-	-	-	-	-
4 ³ A ₁	11.422	-	-	-	-	-	-	-

1
2
3 unfortunately, convergence is not possible. Our approach^{26,56} is therefore to start with a
4 small number of these orbitals and keep adding more, in order of increasing energy, until
5 good agreement is found with the experimental positions of shape resonances. If no exper-
6 mental results are available, the number of VO 'optimized' for a similar molecule is used
7 (for example, for the case of pyridazine, the numbers used for pyrazine and pyrimidine were
8 employed²⁶). This approach tends to under-represent polarization in the CC calculations
9 but provides sufficiently accurate results for an effective comparison with experiments. From
10 this procedure we determine that the optimal number of VOs to include in our SEP and CC
11 calculations was 35 and 70, respectively.
12
13
14
15
16
17
18
19
20
21
22

23 Results

24 Low energy resonances

25
26
27 Our calculations reveal, as expected, the presence of two low-lying π^* resonances, which are
28 characteristic of molecules in which two double bonds are present and that were already
29 identified in earlier experimental and theoretical work.¹³⁻¹⁶ They also reveal the presence of
30 a σ^* resonance, previously identified in calculations.¹⁵ Table 2 lists the positions and widths
31 of these three low-lying resonances determined at SEP and CC level and compares them
32 with the data available in the literature.
33
34
35
36
37
38
39
40

41
42 The positions of the resonances calculated at SEP level agree well with those of da Costa
43 *et al.*¹⁵ calculated at the same level. (Their geometry is slightly different to ours, but, in SE
44 tests, this leads to shifts smaller than 0.1 eV in the resonance positions.) The π^* resonances
45 also agree reasonably with the vertical attachment energies (VAE) determined from the
46 application of the scaled Koopman's theorem using Hartree-Fock orbitals obtained with the
47 6-31G* basis set. The position of the σ^* resonance determined from the VAE is significantly
48 lower than that obtained from SEP scattering calculations. The results of Vinodkumar *et*
49 *al.*¹⁶ overestimate all resonance positions, either because of a poor description of polarization
50
51
52
53
54
55
56
57
58
59
60

Table 2: Positions and widths (in brackets) in eV of the low-lying shape resonances in thiophene taken from our time-delay analysis. The SEP results were calculated for 35 and 41 VO. VAE attachment energies are also presented. We list the calculated results from da Costa *et al.*¹⁵ and Vinodkumar *et al.*¹⁶ and the experimental positions obtained by Asmis¹³ and Modelli and Burrow.¹⁴

Resonances	Present results				Other calc.		Exp.	
	SEP		CC	VAE	¹⁵	¹⁶	¹³	¹⁴
	35 VO	41 VO						
$\pi_1^* (B_1)$	0.949 (0.035)	0.80 (0.020)	1.114 (0.05)	0.95 -	1.00 (0.33)	2.51	1.27	1.15
$\sigma^* (B_2)$	2.990 (2.35)	2.51 (2.107)	~ 1.5 (2.26)	2.11 -	2.78 (1.10)	18.69 -	-	-
$\pi_2^* (A_2)$	2.993 (0.438)	2.87 (0.340)	2.909 (0.48)	3.10 -	2.82 (1.28)	4.35	2.83	2.63

effects or simply because of an incorrect assignation of the resonances.

The positions of the π^* resonances determined experimentally are in good agreement among themselves and with the theoretical results. For reasons explained below, we present SEP R-matrix results, using two different numbers of VO. The effect of increasing the number of VO by 6 is negligible in the A_2 π^* resonance, but lowers the B_1 π^* one by around 0.15 eV and the σ^* resonance by around 0.4 eV.

Prior experience of describing π^* shape resonances in molecules containing a carbon ring^{26,56} indicates that these resonances are better described in SEP calculations where sufficient L^2 configurations can be included to describe polarization. Therefore, it is generally the case in our calculations that the positions of pure π^* shape resonances determined using the CC method are higher than those determined in SEP calculations. When this is not the case, the fact is used to identify the resonances as mixed core-excited shape because it is understood that it is the inclusion of excited states in the close-coupling expansion that improves the description of the resonance and thus lowers its position.^{26,56}

This behaviour is clearly shown by the first π^* resonance (see table 2): our best CC calculation puts it above our best SEP calculation. In the case of the second π^* resonance, SEP and CC calculations seem to give a similar position. However, the σ^* resonance appears

1
2
3 at significantly lower energy in the CC calculation. This behaviour could be interpreted as
4 indicating that the σ^* resonance has mixed character. This is unlikely to be the case for two
5 reasons: (i) the lowest excited state is at 3.7 eV in our calculation, more than 2 eV above
6 this resonance; (ii) being below its excited parent state the resonance could only decay to
7 the ground state. This tends to make resonances longer lived and therefore narrow. The σ^*
8 resonance is more than 2 eV wide.
9
10

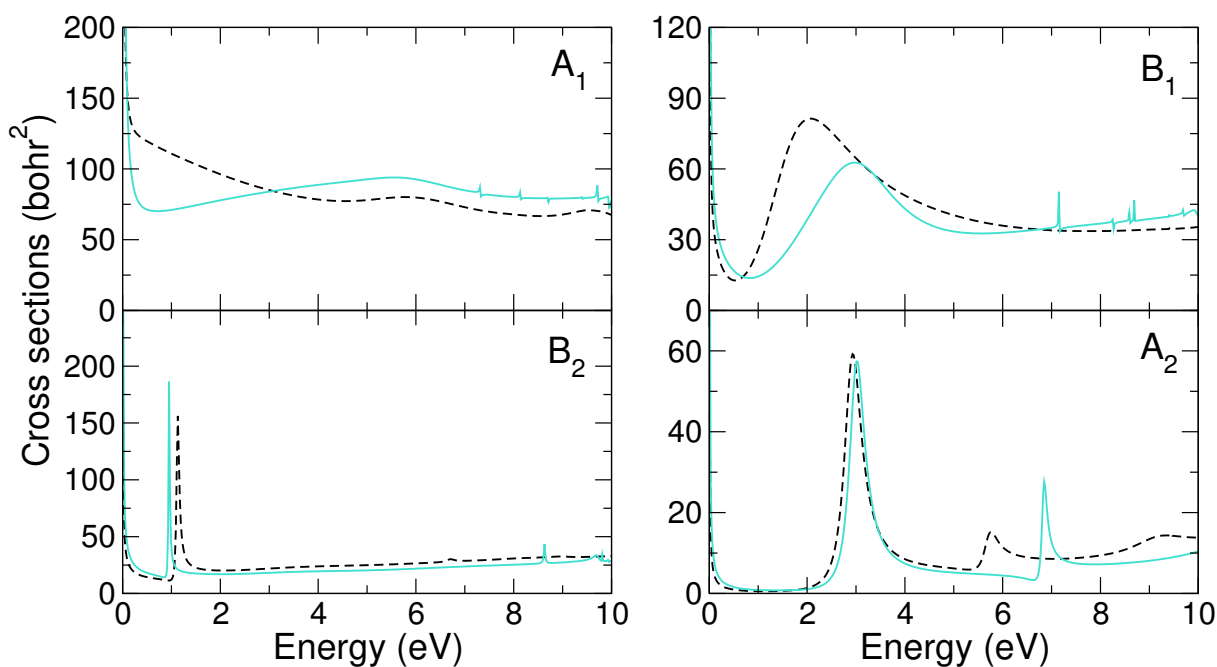
11
12
13 One could argue that this 'unusual behavior' may simply be due to the wrong number
14 of VO being chosen in the calculations. However, the choices presented here lead to π^* reso-
15 nances with positions in very good agreement with experiment. As table 2 shows, increasing
16 the number of VO in the SEP calculation lowers the π^* resonances below their experimental
17 positions. Inclusion of fewer VO in the CC calculation leads either to fairly small changes
18 (if 50 VO are used the upwards shift in the position of all three resonances is of the order of
19 0.2 eV) or a shift that makes agreement for the π^* resonances much worse (when 30 VO are
20 used the σ^* resonance is centred, in the time-delay, around 2.3 eV, however the π^* resonances
21 appear at approximately 1.5 and 3.3 eV).
22
23
24
25
26
27
28
29
30
31
32

33 We believe that our usual recipe (of including more VO until reasonable agreement with
34 experiment for all pure shape resonances is reached) cannot be applied here. This may be due
35 to the fact that, unlike all earlier cases analysed, this target has a mix of σ^* and π^* resonance
36 or due to a more subtle effect. Careful investigation of calculations at SE/SEP and CC level
37 indicated that inclusion of polarization effects has a bigger effect for the σ^* resonance at
38 both levels. However, whereas when polarization is included in an SE calculation (when
39 35 VO are used in the SEP model), the shift is of around 2.4 eV for the σ^* resonance and
40 around 1.8-1.9 eV for the π^* ones, in the CC case (comparing a calculation where no VO
41 are used² to the one with 70 VO) the shift for the σ^* resonance is around 2.5 eV, but for
42 the π^* ones is of 1.2-1.4 eV. It is possible, therefore, that our CC calculation with 70 VO
43 overestimates the polarization effect in the B_2 symmetry placing the σ^* resonance too low in
44
45
46
47
48
49
50
51
52
53

54
55 ²Note that even when no VO are used in the CC calculation, the inclusion of excited states, and L²
56 functions of type (4) already describes some amount of polarization.
57
58
59
60

1
2
3 energy. As a result, we can't conclude confidently where we would expect the σ^* resonance
4 to appear in experiments: Modelli and Burrow's comment¹⁴ would put it closer to the 1.5 eV
5 of our CC calculations, but the calculations of da Costa *et al.* and VEA would indicate a
6 position above 2 eV. It is worth noticing that the maximum of the peak associated to the
7 σ^* resonance in the total cross section calculated at CC level appears around 0.5 eV higher
8 than that in the time-delay. This can be seen in Figure 1 where the contributions to the
9 cross section calculated at SEP and CC level are shown. This is not the case for the SEP
10 calculations, where the difference in position is around 0.1 eV. We believe this indicates the
11 CC calculations are modelling a strong contribution of non-resonant scattering for the 2B_1
12 symmetry that shifts the resonance peak in the cross section.
13
14
15
16
17
18
19
20
21
22

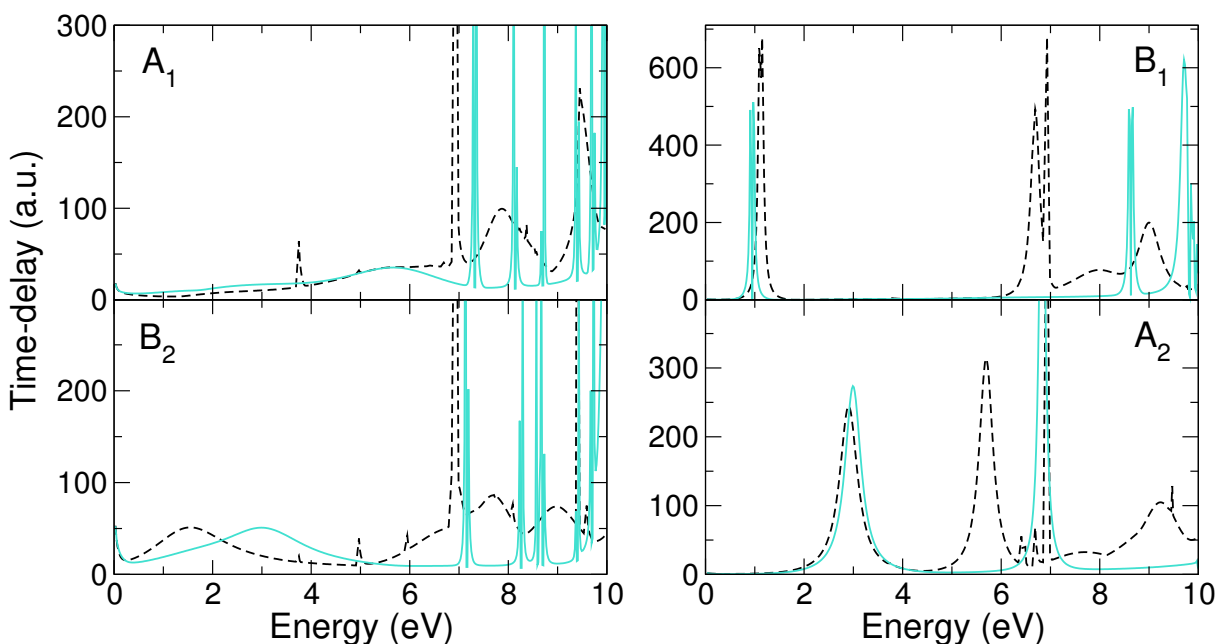
23
24 Figure 1: Contribution to the total cross section from the four irreducible representation of
25 the C_{2v} point group. The dashed black line corresponds to the CC calculation, the solid light
26 blue line corresponds to the SEP calculation with 35 VO. Note that no Born-type correction
27 (see text) has been added to these cross sections.
28



Higher energy resonances

The time-delay obtained at SEP (35 VO) and CC levels is presented in Figure 2. The figure is divided in four panels each corresponding to one of the four irreducible representations of the C_{2v} point group. Above the first excitation threshold, the SEP calculations suffer from the presence of non-physical pseudoresonances (that manifest as narrow peaks appearing above a certain energy), preventing us from providing reliable information on any physical resonances that may appear in that region. One should also notice that all the CC time-delays in Figure 2 have one prominent peak at 6.95 eV, corresponding to one of our excitation thresholds (thresholds are very often visible as narrow peaks/spikes in the time-delay). A summary of the higher resonances found is presented in table 3.

Figure 2: Largest eigenvalue of the time-delay matrix for the scattering symmetries indicated in the panels. The dashed black line corresponds to the CC calculation, the solid light blue line corresponds to the SEP calculation with 35 VO.



The first panel in Figure 2 presents the results for symmetry A_1 . The very narrow peaks in the SEP results are probably pseudoresonances, whereas in the CC calculation we observe two broad peaks corresponding to physical resonances, at 7.9 and 9.5 eV. It is hard to tell whether there are corresponding peaks at SEP level, but since no higher energy resonances

1
2
3 appear in our SE calculation, we believe these are pure core-excited resonances. In addition,
4 a wide structure is visible in the SEP time-delay centred around 5.7 eV. The feature is less
5 obviously present in the CC time-delay, but an analysis of the second largest eigenvalue of the
6 \mathbf{Q} -matrix does indicate a peak centered around a similar energy. A resonance also appears in
7 the SE calculations at ~ 8 eV. Therefore, this feature could correspond to a shape resonance.
8 Investigation of the orbitals that contribute to its description indicate that they have some
9 contribution of CH bond character. The measured excitation function for the first triplet
10 states (see left-hand panel of Figure 3) displays a small band at 4.2 eV to which experimental
11 considerations would assign B_1 symmetry and shape character, although no corresponding
12 structure was found by Asmis. It is possible that this experimental peak corresponds to this
13 resonance, despite the inconsistency in the symmetry.
14

15
16 The different positions of the σ^* resonance calculated at the SEP and CC levels (2.97 and
17 around 1.5 eV respectively), is clearly visible in the panel for the B_2 symmetry. Two other
18 peaks appear in the CC time-delay at around 7.7 and 9 eV. These correspond to core-excited
19 resonances. In addition, there is a feature at ~ 6.9 eV that is hidden in Figure 2 as it overlaps
20 with the peak corresponding to the 7.7 eV resonance, but corresponds to a resonance too.
21 This hypothesis is confirmed by the analysis of the eigenphase sum. No resonances appear in
22 the SE calculation above the σ^* shape resonance, so all the B_2 resonances are of core-excited
23 character. None of them are visible in the total cross section shown in Figure 1.
24

25
26 The upper panel on the right corresponds to the B_1 symmetry. This is where the first
27 π^* resonance appears, at 0.93 and 1.12 eV at the SEP and CC level, respectively. At higher
28 energies, three more resonances are observed in the time-delay analysis: at 6.7 eV, near a
29 threshold, there is a very well defined peak corresponding to a core-excited resonance; a
30 broader feature appears at almost 8 eV with core-excited character; and finally, at 9 eV it
31 is possible to observe a well defined peak. Interestingly, a peak is visible slightly above at
32 SEP level; this peak is much wider than the ones we identify as pseudoresonances, so we
33 believe this peak is likely to be physical. The analysis of the branching ratios indicates that
34
35
36
37
38
39
40
41
42
43
44
45
46
47
48
49
50
51
52
53
54
55
56
57
58
59
60

Table 3: Positions and widths in brackets (in eV) of the higher energy resonances in thiophene. The position of the resonances in the EELS spectra are given as ranges determined from the positions of the peaks in the excitation functions for two angles (see Figure 3). We also list the experimental positions obtained by Asmis.¹³ CE stands for pure core-excited resonances, MCES for mixed core-excited shape resonances and gs for ground state. The most likely Parent States (PS) have been obtained from the branching ratios when possible.

Res.	E_R (width)	Character	PS	EELS	¹³
1^2A_2	5.695 (0.329)	MCES	1^3B_2 , gs	5.4-5.5	5.38
1^2B_1	6.70 (0.172)	CE	$1^3A_1, 1^3B_2$	6.4-6.45	6.22
1^2B_2	6.9 (1.85)	CE	-	-	-
2^2B_2	7.72 (1.15)	CE	1^3A_2	-	-
1^2A_1	7.87 (1.00)	CE	$1^1B_2, 1^1B_1$	-	-
2^2B_1	7.96 (1.20)	MCES	$1^3B_2, 1^3A_1$, gs	7.3-7.5	7.39
3^2B_2	8.98 (1.35)	CE	$1^1B_2, 1^1A_1$	-	-
3^2B_1	9.01 (0.58)	MCES	$1^3B_2, 1^1B_2$, gs	-	-
2^2A_2	9.22 (0.95)	CE	$1^3A_1, 2^3A_1, 1^3B_2$	8.0-8.1	7.93
2^2A_1	9.48 (0.2)	CE	$1^3A_2, 1^1A_2$	-	-

1
2
3 all these resonances have mixed shape core-excited character. Again, the resonances are not
4 visible in the total cross section.
5
6

7 Finally, the A_2 symmetry presented in the last panel shows the second shape π^* res-
8 onance discussed earlier (see table 2). A second resonance present around 5.7 eV in the
9 CC calculation has its corresponding peak at the SEP level appearing almost 1 eV higher.
10 One other resonance, of core-excited character, is located at 9.2 eV. The structure (looking
11 like truncated peaks) between 6 and 7 eV is hard to discern: it may just correspond to the
12 thresholds or be linked to Feshbach resonances. Our calculations, however, do not identify
13 any Feshbach resonances.
14
15
16
17
18
19
20

21 Table 3 summarizes the resonance positions and widths for the CC calculation, as well as
22 the positions obtained from the experimental excitation functions (see below). The resonance
23 positions are in good agreement with Asmis.¹³ Although Vinodkumar *et al.* present data
24 for a number of core-excited resonances, we have chosen not to include their results in the
25 table as it is fairly clear that they are incorrect: all their core-excited resonances appear well
26 above (between 3 and 10 eV) the ionization threshold. This can be directly linked to the
27 fact that, in their work, the excitation energies of the parent states are much higher than in
28 experiments. An inadequate description of polarization effects may also be contributing to
29 the poor quality of Vinodkumar *et al.*'s results.
30
31
32
33
34
35
36
37
38
39
40

41 **Excitation functions**

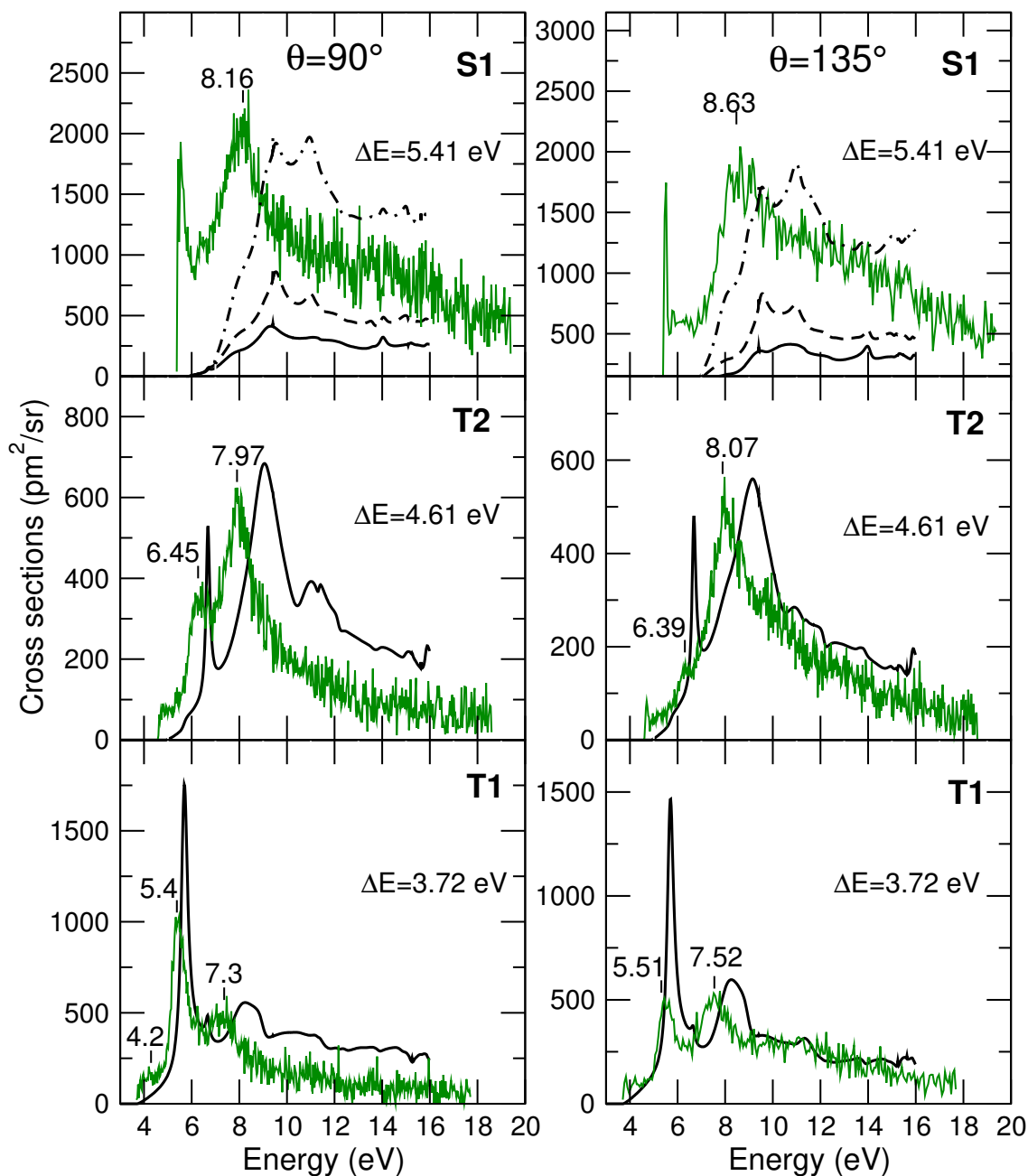
42
43 The experimental and theoretical excitation functions for two different electron scattering
44 angles, 90° and 135° , are presented in Figure 3. Our energy loss spectra (see the supporting
45 information) place the first triplet state (1^3B_2 , T1) at 3.72 eV, the second (1^3A_1 , T2) at
46 4.61 eV and the first singlet state (1^1A_1 , S1) at 5.41 eV. For this reason, the excitation
47 functions were measured for energy losses, ΔE , of 3.72 eV, 4.61 eV and 5.41 eV. However,
48 the band centered around ~ 5.6 eV in energy loss for 135° shows the likely presence of other
49 triplet state (or states) that partly overlap with the S1 state. Therefore the excitation
50
51
52
53
54
55
56
57
58
59
60

1
2
3 function labelled S1 actually corresponds to the excitation of several states of thiophene,
4 though it is difficult to determine which and how many. We have therefore plotted three
5 calculated curves for the $\Delta E=5.41$ eV energy loss: one (solid black line) corresponding
6 to the excitation into the lowest singlet excited state (S1) only, another one (dashed line)
7 corresponding to the excitations into the S1 state plus the third and fourth triplet states in
8 our calculations (1^3B_1 and 1^3A_2) and finally one (dotted-dashed line) where excitations into
9 the third, fourth, fifth and sixth triplet states plus the first, third and fourth singlet states
10 in our calculations are added together (the second singlet state in our calculations appears
11 at higher energy than our fourth, and sometimes our third, in more accurate calculations).
12
13
14
15
16
17
18
19
20

21 The size and shape of the measured and calculated excitation functions for $\Delta E=3.72$ and
22 4.61 eV agree extremely well. This agreement is similar to that obtained for pyrimidine,³³
23 but in that case the quantity compared was integral excitation cross sections (obtained from
24 the integration over all angles of the excitation functions). Here, we show the agreement
25 to be excellent for specific angles. For $\Delta E=5.41$ eV, the agreement is not as good: it
26 is clear that inclusion of three states in the calculation produces an excitation function
27 that is much smaller than the experimental one. One needs to include at least 7 states
28 to obtain a calculated cross section of similar size to the experimental one. This does
29 not necessarily indicate that all these 7 states contribute to this excitation function. The
30 quality of description of the electronic states of thiophene in our calculations gets worse as
31 their energy increases, in part, but not only, because some of these states have Rydberg
32 character. Therefore, the calculations will clearly provide a less accurate description of
33 electronic excitation into higher-lying states. It is this effect that may be leading to an
34 inaccurate excitation function for $\Delta E=5.41$ eV and the need to include more states than are
35 actually contributing to the measurement.
36
37
38
39
40
41
42
43
44
45
46
47
48
49
50

51 The positions of those resonances identified in the excitation functions show good agree-
52 ment with our calculated resonances. As expected, the calculated resonance positions are
53 at higher energies than the experimental ones. There may be two reasons for this: first,
54
55
56
57
58
59
60

Figure 3: Calculated (black lines) and measured (green line) excitation functions for the energy losses indicated in the panels: left panels, scattering angle of 90° ; right panels scattering angle of 135° . The peaks of the measured excitation functions are also indicated in the panels. For $\Delta E=5.41$ eV, the full black line corresponds to excitation into the first excited singlet state only, whereas the dashed and dotted-dashed lines correspond to the sum of excitations into 3 and 7 states respectively. See text for more details.



the energies of the parent states are overestimated in our calculation, and second, it is expected that the polarization effects will not be fully described in a CC calculation. The

1
2
3 latter is likely to be a smaller effect for thiophene, as the shape resonances are in fairly good
4 agreement with experiment. A similar comparison for pyrimidine³³ produced very similar
5 agreement (including the absence of some calculated resonances in the EELS cross sections):
6
7 the shifts are somewhat smaller in this case but, as for pyrimidine, increase as the resonance
8 energy increases.
9
10

11
12
13 It is not surprising that some of the resonances identified in our calculations cannot be
14 seen in the EELS experiments: not all core-excited resonances have a strong effect in the
15 electronic excitation cross sections. Those calculated resonances that are visible appear, as
16 expected, in the excitation function of their parent states: the 1^2A_2 one appears in the T1,
17 the 1^2B_1 appears both in T1 and T2, the 2^2B_1 appears again in both T1 and T2 and the 2^2A_2
18 appears in all three. Of the resonances that are not apparent in the experimental excitation
19 functions, only the 3^2B_1 (at around 9 eV in our calculations) has either the T1, T2 or S2 as
20 the main parent state (specifically, the T1).
21
22
23
24
25
26
27
28
29
30

31 Comparison with DEA results

32
33 The DEA experiments Muftakhov *et al.* are hard to correlate to the resonances we identified,
34 but some links can be made. The ion yields for H-loss and the formation of a fragment with
35 mass 32 have a peak around 3.4-3.5 eV. The only possible resonance on our calculations
36 this may be linked to is the higher-lying pure shape π^* resonance located around 2.9 eV.
37 Alternatively, the peak in these yields could correspond to a narrow Feshbach resonance
38 that we have failed to identify whose parent is the lowest excited state (the 1^3B_2). The ion
39 yields for several fragments (among them the one coming from single H-loss) display peaks
40 at around 5.3, 5.5 and 5.8 eV. Again, the only resonance we describe in our calculations that
41 could be linked to these peaks is the 1^2A_2 at ~ 5.7 eV seen by the EELS closer to 5.4-5.5 eV.
42 Peaks in the mass spectra in the range 6.15-6.4 eV could be linked to the 1^2B_1 resonance
43 we observe at 6.7 eV and the EELS puts at 6.4-6.45 eV (the 1^2B_2 resonance around 6.9 eV
44 is much shorter lived so less likely to lead to dissociation). Finally, several peaks in the
45
46
47
48
49
50
51
52
53
54
55
56
57
58
59
60

1
2
3 8.5-8.9 eV range could be linked to one or several of the resonances we describe in the 8.98
4 to 9.45 eV range. Muftakhov *et al.* do not report peaks in the mass spectra below 3.3 eV.
5
6
7
8

9 **Conclusions**

10
11
12 We have performed R-matrix calculations and EELS experiments for electron scattering from
13 thiophene in order to identify and characterize its core-excited resonances. Comparison of
14 measured and calculated excitation functions for two different angles and three different
15 energy losses show very good agreement: both their size and shape agree very well, at least
16 for the two energy losses where it is clear which states are being excited. This indicates that
17 the calculations are modelling the physics of the collision accurately, despite the fact that
18 our usual strategy for determining how to model the polarization effects (i.e. how many
19 virtual orbitals are required for their description) does not seem to work particularly well for
20 this system. It also demonstrates that it is now possible to provide quantitatively accurate
21 cross sections for low energy electronic excitation of low-lying states of biologically relevant
22 molecules.
23
24
25
26
27
28
29
30
31
32
33

34
35 Our calculated results for the pure shape resonances agree well with previous calculations
36 and experiments, although some uncertainty persists as to the accurate position of the rather
37 wide σ^* resonance. Four core-excited or mixed core-excited resonances described by our
38 calculations are visible in the excitation functions although, as expected, the calculated ones
39 appear higher in energy. These are, on the whole, the longer lived (i.e. narrower) resonances
40 identified. A feature appears around 4.2 eV in the excitation function that we believe may
41 correspond to a poorly described (in the calculations) pure shape A_1 resonance. Another
42 six resonances are identified in our calculations. Finally, some of the core-excited resonances
43 can be linked to the DEA spectra of Muftakhov *et al.*¹²
44
45
46
47
48
49
50
51
52
53
54
55
56
57
58
59
60

Acknowledgement

This work used the ARCHER UK National Supercomputing Service (<http://www.archer.ac.uk>). MA and KR acknowledge support by the project No. 200020-144367/1 of the Swiss National Science Foundation. AL was supported by Fundação para a Ciência e a Tecnologia (FCT-MCTES), Radiation Biology and Biophysics Doctoral Training Programme (RaBBiT, PD/00193/2012); UID/Multi/04378/2013 (UCIBIO); UID/FIS/00068/2013 (CEFITEC). KR acknowledges the Swiss National Science Foundation for an EPM fellowship.

Supporting Information Available

Energy loss spectra measured in the forward and backward directions in order to identify the excited states of thiophene. Experimental elastic differential cross sections.

References

- (1) Boudaïffa, B.; Cloutier, P.; Hunting, D.; Huels, M. A.; Sanche, L. Resonant Formation of DNA Strand Breaks by Low-energy (3 to 20 eV) Electrons. *Science* **2000**, *287*, 1658–1660.
- (2) Fabrikant, I. I.; Eden, S.; Mason, N. J.; Fedor, J. In *Advances in atomic, molecular, and optical physics*; Ennio Arimondo, C. C. L., Yelin, S. F., Eds.; Advances In Atomic, Molecular, and Optical Physics; Academic Press, 2017; Vol. 66; pp 545 – 657.
- (3) Alizadeh, E.; Sanche, L. Precursors of Solvated Electrons in Radiobiological Physics and Chemistry. *Chem. Rev.* **2012**, *112*, 5578–5602.
- (4) Baccarelli, I.; Bald, I.; Gianturco, F. A.; Illenberger, E.; Kopyra, J. Electron-induced Damage of DNA and its Components: Experiments and Theoretical Models. *Phys. Rep.* **2011**, *508*, 1–44.

- 1
2
3 (5) Gorfinkiel, J. D.; Ptasińska, S. Electron Scattering from Molecules and Molecular Ag-
4 gregates of Biological Relevance. *J. Phys. B* **2017**, *50*, 182001.
5
6
7
8 (6) Gramec, D.; Peterlin, L.; Sollner, M. Bioactivation Potential of Thiophene-containing
9 Drugs. *Chem. Res. Toxicol.* **2014**, *8*, 1344–1358.
10
11
12 (7) Hedhili, M. N.; Cloutier, P.; Bass, A. D.; Madey, T. E.; Sanche, L. Electron Stim-
13 ulated Desorption of Anionic Fragments from Films of Pure and Electron-irradiated
14 Thiophene. *J. Chem. Phys.* **2006**, *125*, 094704.
15
16
17
18
19 (8) Staykov, A.; Areephong, J.; W.Browne,; Feringa, B.; Yoshizawa, K. Electrochemical
20 and Photochemical Cyclization and Cycloreversion of Diarylethenes and Diarylethene-
21 capped Sexithiophene Wires. *ACS Nano* **2011**, *5*, 1165–1178.
22
23
24
25
26 (9) Dimitrakopolous, C.; Malenfant, P. Organic Thin Film Transistors for Large Area Elec-
27 tronics. *Adv. Mater.* **2002**, *14*, 99–117.
28
29
30
31 (10) Liang, Y.; Yu, L. Development of Semiconducting Polymers for Solar Energy Harvest-
32 ing. *Polym. Rev.* **2010**, *50*, 454–473.
33
34
35
36 (11) Murphy, A.; Frechet, J. Organic Semiconducting Oligomers for Use in Thin Film Tran-
37 sistors. *Chem. Rev.* **2007**, *107*, 1066–1096.
38
39
40
41 (12) Muftakhov, M. V.; Asfandiarov, N.; Khvostenko, V. I. Resonant Dissociative Electron
42 Attachment of Electrons to Molecules of Five-membered Heterocyclic Compounds and
43 Lactams. *J. Electron. Spectrosc. Relat. Phenom.* **1994**, *69*, 165–175.
44
45
46
47 (13) K.R.Asmis, Ph.D. thesis, Université de Fribourg, Switzerland, 1996.
48
49
50 (14) Modelli, A.; Burrow, P. Electron Attachment to the Aza-derivatives of Furan, Pyrrole
51 and Thiophene. *J. Chem. Phys. A* **2004**, *108*, 5721–5726.
52
53
54
55 (15) da Costa, R.; do N. Varella, M.; Lima, M.; Bettega, M. Low-energy Electron Collisions
56 with Thiophene. *J. Chem. Phys.* **2013**, *138*, 194306.
57
58

- 1
2
3 (16) Vinodkumar, M.; Desai, H.; Vinodkumar, P. Electron Induced Chemistry of Thiophene.
4 *RSC Adv.* **2015**, *5*, 24564–24574.
5
6
7
8 (17) Mozejko, P.; Ptasinska-Denga, E.; Szymtkowski, C. Cross Sections for Electron Collision
9 with Five-membered Ring Heterocycles. *Eur. Phys. J. D* **2012**, *66*, 20659–20666.
10
11
12 (18) Tennyson, J. Electron-molecule Collision Calculations Using the R-matrix Method.
13 *Phys. Rep.* **2010**, *491*, 29–76.
14
15
16
17 (19) Carr, J. M.; Galiatsatos, P. G.; Gorfinkiel, J. D.; Harvey, A. G.; Lysaght, M. A.;
18 Madden, D.; Mašín, Z.; Plummer, M.; Tennyson, J.; Varambhia, H. N. UKRmol: a
19 Low-energy Electron- and Positron-molecule Scattering Suite. *Eur. Phys. J. D* **2012**,
20 *66*, 20653–20656.
21
22
23
24
25
26 (20) Burke, P. G. *R-matrix Theory of Atomic Collisions: Application to Atomic, Molecular*
27 *and Optical Processes*; Springer, 2011.
28
29
30
31 (21) Fabrikant, I. I. Long-range Effects in Electron Scattering by Polar Molecules. *J. Phys.*
32 *B* **2016**, *49*, 222005.
33
34
35
36 (22) Mašín, Z.; Gorfinkiel, J. D.; Jones, D. B.; Bellm, S. M.; Brunger, M. J. Elastic and
37 Inelastic Cross Sections for Low-energy Electron Collisions with Pyrimidine. *J. Chem.*
38 *Phys.* **2012**, *136*, 144310–144320.
39
40
41
42 (23) Norcross, D. W.; Padiál, N. T. The Multipole-extracted Adiabatic-nuclei Approxima-
43 tion for Electron-molecule Collisions. *Phys. Rev. A* **1982**, *25*, 226–238.
44
45
46
47 (24) Tashiro, M.; Morokuma, K.; Tennyson, J. R-matrix Calculation of Differential Cross
48 Sections for Low-energy Electron Collisions with Ground-state and Electronically
49 Excited-state O₂ Molecules. *Phys. Rev. A* **2006**, *74*, 022706–022714.
50
51
52
53
54 (25) Hazi, A. U. Behavior of the Eigenphase Sum Near a Resonance. *Phys. Rev. A* **1979**,
55 *19*, 920–922.
56
57
58
59
60

- 1
2
3 (26) Mašín, Z.; Gorfinkiel, J. D. Shape and Core Excited Resonances in Electron Collisions
4 with Diazines. *J. Chem. Phys.* **2012**, *137*, 204312.
5
6
7
8 (27) Shimamura, I.; Cleanthes, E.; Nicolaides, A.; Sabin, J. *Advances in Quantum Chem-*
9 *istry*; Academic, 2012.
10
11
12
13 (28) Smith, F. T. Lifetime Matrix in Collision Theory. *Phys. Rev.* **1960**, *118*, 349–356.
14
15
16 (29) Allan, M.; Winstead, C.; McKoy, V. Electron Scattering in Ethene: Excitation of the
17 \tilde{a}^3B_{1u} State, Elastic Scattering and Vibrational Excitation. *Phys. Rev. A* **2008**, *77*,
18 042715.
19
20
21
22 (30) Allan, M. Electron Collisions with CO: Elastic and Vibrational Excitation Cross Sec-
23 tions. *Phys. Rev. A* **2010**, *81*, 042706.
24
25
26
27 (31) Regeta, K.; Allan, M. Absolute Cross Sections for Electronic Excitation of Furan by
28 Electron Impact. *Phys. Rev. A* **2015**, *91*, 012707.
29
30
31
32 (32) Regeta, K.; Allan, M.; Winstead, C.; McKoy, V.; Mašín, Z.; Gorfinkiel, J. D. Resonance
33 Effects in Elastic Cross Sections for Electron Scattering on Pyrimidine: Experiment and
34 Theory. *J. Chem. Phys.* **2016**, *144*, 024301.
35
36
37
38 (33) Regeta, K.; Allan, M.; Mašín, Z.; Gorfinkiel, J. D. Absolute Cross Sections for Electronic
39 Excitation of Pyrimidine by Electron Impact. *J. Chem. Phys.* **2016**, *144*, 024302.
40
41
42
43 (34) Gopalan, A.; Bömmels, J.; Götte, S.; Landwehr, A.; Franz, K.; Ruf, M. W.; Hotop, H.;
44 Bartschat, K. A Novel Electron Scattering Apparatus Combining a Laser Photoelectron
45 Source and a Triply Differentially Pumped Supersonic Beam Target: Characterization
46 and Results for the $\text{He}^-(1s2s^2)$ Resonance. *Eur. Phys. J. D* **2003**, *22*, 17–29.
47
48
49
50 (35) Allan, M. Measurement of the Elastic and $v = 0 \rightarrow 1$ Differential Electron- N_2 Cross
51 Sections Over a Wide Angular Range. *J. Phys. B: At. Mol. Opt. Phys.* **2005**, *38*, 3655–
52 3672.
53
54
55
56
57
58
59
60

- 1
2
3
4 (36) Nickel, J. C.; Zetner, P. W.; Shen, G.; Trajmar, S. Principles and Procedures for
5 Determining Absolute Differential Electron-molecule (Atom) Scattering Cross Sections.
6 *J. Phys. E: Sci. Instrum.* **1989**, *22*, 730–738.
7
8
9
10 (37) Nesbet, R. K. Variational Calculations of Accurate e^- –He Cross Sections Below 19 eV.
11 *Phys. Rev. A* **1979**, *20*, 58–70.
12
13
14 (38) McClellan, A. *Tables of experimental dipole moments*; W.H.Freeman, 1963.
15
16
17 (39) Gussoni, M.; Rui, R.; Zerbi, G. Electronic and Relaxation Contribution to Linear Molec-
18 ular Polarizability. An Analysis of the Experimental Values. *J. Mol. Struct.* **1998**, *447*,
19 163–215.
20
21
22 (40) Editor, R. D. J. I. NIST Standard reference database. [http://http://cccbdb.nist.](http://cccbdb.nist.gov)
23 [gov](http://cccbdb.nist.gov), Accessed: 2017-10-04.
24
25
26 (41) Palmer, M. H.; Walker, I. C.; Guest, M. F. The Electronic States of Thiophene Stud-
27 ied by Optical (VUV) Absorption, Near-threshold Electron Energy Loss (EEL) Spec-
28 troscopy and Ab Initio Multi-Reference Configuration Interaction Calculations. *Chem.*
29 *Phys.* **1999**, *241*, 275–296.
30
31
32 (42) Haberkern, H.; Asmis, K.; Allan, M.; Swiderek, P. Triplet States in Oligomeric Mate-
33 rials: Electron Energy Loss Spectroscopy of Thiophene and Bithiophene and Extrapo-
34 lation to the Polymer. *Phys. Chem. Chem. Phys.* **2003**, *5*, 827–833.
35
36
37 (43) Flicker, W.; Mosher, O.; Kupperman, A. Electron Impact Investigation of Electronic
38 Excitations in Furan, Thiophene, and Pyrrole. *J. Chem. Phys.* **1976**, *64*, 1315–1321.
39
40
41 (44) Salzmann, S.; Kleinschmidt, M.; Weinkauf, J. T. R.; Marian, C. M. Excited States
42 of Thiophene: Ring Opening as Deactivation Mechanism. *Phys. Chem. Chem. Phys.*
43 **2008**, *10*, 380–392.
44
45
46
47
48
49
50
51
52
53
54
55
56
57
58
59
60

- 1
2
3 (45) Weinkauff, R.; Lehr, L.; Schlag, E. W.; Salzmann, S.; Marian, C. M. Ultrafast Dynamics
4 in Thiophene Investigated by Femtosecond Pump Probe Photoelectron Spectroscopy
5 and Theory. *Phys. Chem. Chem. Phys.* **2008**, *10*, 393–404.
6
7
8
9
10 (46) Holland, D. M. P.; Trofimov, A. B.; Seddon, E. A.; Gromov, E. V.; Korona, T.;
11 de Oliveira, N.; Archer, L. E.; Joyeux, D.; Nahon, L. Excited Electronic States of
12 Thiophene: High Resolution Photoabsorption Fourier Transform Spectroscopy and *Ab*
13 *Initio* Calculations. *Phys. Chem. Chem. Phys.* **2014**, *16*, 21629–21644.
14
15
16
17
18 (47) Wan, J.; Hada, M.; Ehara, M.; Nakatsuji, H. Electronic Excitation Spectrum of Thio-
19 phene Studied by Symmetry-adapted Cluster Configuration Interaction Method. *J.*
20 *Chem. Phys.* **2001**, *114*, 845–850.
21
22
23
24
25 (48) Serrano-Andrés, L.; Merchán, M.; Fulscher, M.; Roos, B. O. A Theoretical Study of
26 the Electronic Spectrum of Thiophene. *Chem. Phys. Lett.* **1993**, *211*, 125–134.
27
28
29
30 (49) Kleinschmidt, M.; Tatchen, J.; Marian, C. Spin-orbit Coupling of DFT/MRCI Wave-
31 functions: Method, Test Calculations, and Application to Thiophene. *J. Comput.*
32 *Chem.* **2002**, *23*, 824–833.
33
34
35
36
37 (50) Werner, H.-J.; Knowles, P. J.; Knizia, G.; Manby, F. R.; Schütz, M.; Celani, P.;
38 Györffy, W.; Kats, D.; Korona, T.; Lindh, R. et al. MOLPRO, version 2015.1, a package
39 of ab initio programs. 2015; see <http://www.molpro.net>.
40
41
42
43
44 (51) Jones, E.; I.M.Moodie, The Synthesis and Absorption Spectra of the Isomeric Dithienyl
45 Sulphides. *Tetrahedron* **1965**, *21*, 2413–2420.
46
47
48
49 (52) Leonardo, G. D.; Galloni, G.; Trombetti, A.; Zauli, C. Electronic Spectrum of Thiophen
50 and Some Deuterated Thiophens. *J. Chem. Soc. Faraday Trans* **1972**, *68*, 2009–2016.
51
52
53
54 (53) Veen, E. H. V. Triplet $\pi - \pi^*$ Transitions in Thiophene, Furan and Pyrrole by Low-
55 energy Electron Impact Spectroscopy. *Chem. Phys. Lett.* **1976**, *41*, 535–539.
56
57
58
59
60

- 1
2
3 (54) Nyulászy, L.; Veszprémi, T. Near Ultraviolet Spectrum of Thiophene and its Deriva-
4 tives. *Chem. Scr.* **1986**, *26*, 629–634.
5
6
7
8 (55) Hakanson, R.; Nordén, B.; Thulstrup, E. Magnetic Circular Dichroism of Heterocycles:
9 Thiophene. *Chem. Phys. Lett.* **1977**, *50*, 306–308.
10
11
12
13 (56) Loupas, A.; Gorfinkiel, J. D. Resonances in Low-energy Electron Scattering from para-
14 Benzoquinone. *Phys. Chem. Chem. Phys.* **2017**, *19*, 18252–18261.
15
16
17
18
19
20
21
22
23
24
25
26
27
28
29
30
31
32
33
34
35
36
37
38
39
40
41
42
43
44
45
46
47
48
49
50
51
52
53
54
55
56
57
58
59
60

Graphical TOC Entry

